J Neuropathol Exp Neurol
Vol. 65, No. 5
May 2006
pp. 433–444
Copyright © 2006 by the American Association of Neuropathologists, Inc.

ORIGINAL ARTICLE

Nogo-A Expression in the Human Hippocampus in Normal Aging and in Alzheimer Disease

Vanessa Gil, Oriol Nicolas, Ana Mingorance, Jesús Mariano Ureña, PhD, Bor Lueng Tang, PhD, Tatsumi Hirata, PhD, Javier Sáez-Valero, PhD, Isidro Ferrer, MD, PhD, Eduardo Soriano, PhD, and José Antonio del Río, PhD

Abstract

Myelin-associated proteins are involved in the formation and stabilization of myelin sheaths. In addition, they prevent axon regeneration and plasticity in the adult brain. Recent evidence suggests that the expression of certain myelin-associated proteins (e.g. Nogo-A) can be regulated by synaptic activity or by overexpression after neural lesions in brain syndromes such as temporal lobe epilepsy. However, no studies on Alzheimer disease (AD) have been reported in which cell loss and significant synaptic reorganization occurs. In the present study, we analyze in detail the expression of Nogo-A in the hippocampal formation in normal human aging and in AD. Our results indicate that Nogo-A is expressed by oligodendrocytes and neurons in the aged hippocampal formation. In addition, both granule cells and mossy fiber connections are also labeled in the old-aged hippocampi. Interestingly, Nogo-A is over-expressed by hippocampal neurons in AD and is associated with β-amyloid deposits in senile plaques. Taken together, our results reinforce the hypothesis that Reticulon proteins such as Nogo-A participate in the neuronal responses stemming from hippocampal formation during senescence, and particularly in AD. These findings also indicate that Reticulon proteins could be considered as new putative drug targets in therapies of neurodegenerative disorders.

Key Words: Alzheimer disease, Human hippocampus, Myelin-associated proteins, Nogo-A.

From Development and Regeneration of the CNS (VG, ON, AM, JMU, ES, JADR), IRB-PCB, Barcelona Science Park, University of Barcelona, Spain; Department of Biochemistry (BLT), National University of Singapore, Republic of Singapore; Division of Brain Function (TH), National Institute of Genetics, Graduate University for Advanced Studies, Japan; Instituto de Neurociencias de Alicante (JSV), Universidad Miguel Hernández-CSIC, Spain; and Institute of Neuropathology (IF), Faculty of Medicine, IDIBELL-Hospital Universitari de Bellvitge, University of Barcelona, Spain.

Grant support provided by the Spanish Ministry of Science and Technology (MCYT; EET2002-05149 and BFI2003-03594) and the Caixa Foundation to JADR; and SAF2004-07929 to ES. ON is a predoctoral fellow of the Ramón Areces Foundation, and VG and AM are predoctoral fellows of the Spanish Ministry of Education and Science.

Send correspondence and reprint requests to: José Antonio del Río, PhD, Development and Regeneration of the CNS, Department of Cell Biology-IRB, Barcelona Science Park, Universitat de Barcelona, Josep Samitier 1-5; E-08028, Barcelona, Spain; E-mail: jario@pcb.ub.es or jrio@ub.edu

Supplementary data is available online at http:www.jneuropath.com.

INTRODUCTION

Alzheimer disease (AD) is characterized by the presence of neuritic and cerebrovascular plaques containing β-amyloid (Aβ) peptides, neurofibrillary tangles enriched in hyperphosphorylated tau protein, activation of glial cells, and neuronal degeneration (1–3). Numerous studies have reported that fibrillar Aβ peptides are toxic to several cell types, including cultured neurons in vitro (4) and in vivo (5), endothelial cells (6), and glial cells (7). Oligodendrocytes are particularly reactive and vulnerable to oxidative stress, inflammatory cytokines, and excitotoxic neurotransmitters, all of which cause injury in AD-affected brains (8). Hence, the degeneration of oligodendrocytes may correlate with the loss of myelinated axonal tracts described in AD (9, 10). The loss of oligodendrocytes might have deleterious effects on neuronal viability, since they express multiple growth factors in the normal brain (11–13).

Several myelin-associated proteins involved in the formation and maintenance of myelin sheaths also prevent axonal regeneration and plasticity in the adult mammalian CNS (14). To date, 3 myelin inhibitors with these functions have been characterized: Nogo-A (15–17), myelin-associated glycoprotein (MAG) (18, 19), and oligodendrocyte-myelin glycoprotein (OMgp) (20, 21). Nogo-A contains 200 amino acids in its C-terminal region, which is homologous to members of the Reticulon (*Rtn*) gene family (22). All 3 myelin-derived molecules share a common neuronal receptor complex comprising NgR, p75, TAJ-1/TROY, and LINGO-1 (23-26). Studies using α-Nogo antibodies have shown that most Nogo proteins in oligodendrocytes and neurons are localized to the endoplasmic reticulum, with only a low percentage found in the cell membrane (17, 27–29).

Several studies have described the presence of Nogo-A and NgR mRNAs and proteins in the human brain, both during development (30–32) and in the adulthood (33, 34).However, characterization of Nogo-A-immunoreactive cell types in the adult hippocampus has led to conflicting results (33, 34). Although the function of Nogo-A in neurons is largely unknown, it has been implicated in synaptic plasticity following CNS injuries in rodents (35–39). In addition, recent findings indicate that cell expression of certain myelin-associated proteins can be modified in several brain pathologies. Indeed, increased levels of Nogo-A have been described in patients with temporal lobe epilepsy (34)

Downloaded from http://jnen.oxfordjournals.org/ by guest on October 8, 2016

Copyright © 2006 by the American Association of Neuropathologists, Inc. Unauthorized reproduction of this article is prohibited.

and in multiple sclerosis (40). Increased Nogo-A mRNA levels have been reported in schizophrenia (41–43). In spite of these studies, no data are available on AD, in which increased myelin-basic protein (MBP) mRNA levels have been described in affected brains, in parallel with losses of myelin tracts (44, 45). The hippocampal formation (HF) is an early and one of the most severely affected brain areas in AD (1). With this in mind, we examined the expression of Nogo-A in human HF in both normal aging and AD. We provide evidence that Nogo-A is expressed in the adult human hippocampus by principal and local-circuit neurons, as well as by oligodendrocytes. Surprisingly, Nogo-A immunoreactivity is also observed in granule cells and their projecting axons in old-aged brains. Moreover, a relevant increase in Nogo-A expression is found in pyramidal neurons of both the HF and the neocortex in AD and is also localized in senile plaques around amyloid deposits that were also surrounded by reactive astrocytes. Taken together, these results not only indicate that Nogo-A is upregulated in the AD hippocampus, but also reinforce the hypothesis that Nogo-A plays a role in synaptic plasticity and functional reorganization in certain brain diseases.

MATERIALS AND METHODS

AD and Non-AD Cases

This study is based on 14 non-AD and 16 AD postmortem human brains from the Institute of Neuropathology and University of Barcelona/Hospital Clinic Brain Banks. All brains were obtained within 2 to 13 hours after death, following

TABLE. AD and Non-AD Cases Examined in the Present Study

Patient ID	Age (y), Sex	Time Postmortem (h)	Cortical region	Post-fixation time (d)	Type of investigation
Non-AD					
nAD_{68}	51, M	4	HF	1	IHC
nAD_{22}	52, M	4	HF	15	IHC
nAD_{34}	53, M	3	HF	1	IHC
nAD_{85}	55, M	7	HF	1	IHC
nAD_{25}	65, F	4	HF + FC	1	IHC
nAD_{183}	71, F	2.4	FC	1	IHC
nAD_{65}	73, F	7	HF	1	IHC
nAD_{100}	80, F	3.30	HF	1	IHC
nAD_{05}	58, M	4	HF		WB
nAD_{180}	69, F	2.3	HF		WB
nAD_{352}	70, F	5	FC		WB
$nAD_{03/3}$	71, F	7	FC		WB
$nAD_{27/02}$	74, M	6.15	FC		WB
$nAD_{71/02}$	76, F	5	FC		WB
AD					
AD_{63}	68, M	4.45	HF + FC	1	IHC
AD_{149}	69, M	4	HF	15	IHC
AD_{122}	75, M	4	HF	15	IHC
AD_{157}	79, M	4.45	HF	1	IHC
AD_{148}	83, F	4	HF	1	IHC
AD_{173}	83, F	5	HF	1	IHC
AD_{48}	84, F	2	FC	1	IHC
AD_{433}	67, M	7.3	FC		WB
AD_{438}	67, M	2.3	FC		WB
AD_{440}	72, M	7.3	FC		WB
AD_{430}	77, F	6.15	FC		WB
AD_{657}	77, M	6	HF		WB, IP
$AD_{41/02}$	78, M	7	FC		WB
AD_{710}	80, M	13	HF		WB, IP
AD_{429}	81, F	3.3	FC		WB
AD_{713}	90, M	4.30	HF		WB, IP
Epileptic					
E_{240}	65*, M	-	HF		IHC
E_{241}	43*, F	-	HF		IHC

E, samples from epileptics with sclerotic hippocampi; y, years; *, age at the time of surgery; M, male; F, female; h, hours; HF, hippocampal formation; FC, frontal cortex; d, days; IHC, Immunohistochemistry; WB, Western blot; IP, immunoprecipitation.

© 2006 American Association of Neuropathologists, Inc.

Downloaded from http://jnen.oxfordjournals.org/ by guest on October 8, 2016

Copyright © 2006 by the American Association of Neuropathologists, Inc. Unauthorized reproduction of this article is prohibited.

the Code of Ethics of the World Medical Association and the protocols of the local ethical committee. Basic patient data are shown in the Table. Clinically, 16 patients had suffered from severe dementia of Alzheimer type following the diagnostic criteria of the NINCDS-ADRDA, and all of them had a clinical dementia rating scale (CDR) stage 3 (46). Fourteen cases were neurologically normal. Cases with and without clinical neurological disease were processed in the same way following the same sampling and staining protocols. At autopsy, half of each brain was fixed in 10% buffered formalin, while the other half was cut in coronal sections 1-cm thick, frozen on dry ice, and stored at −80°C until use. In addition, 2-mm-thick samples of the cerebral isocortex, cingulum, hippocampus and entorhinal cortex, and brainstem were fixed with 4% paraformaldehyde for 24 hours, cryoprotected with 30% sucrose, frozen on dry ice, and stored at −80°C until use. Following neuropathological examination, AD cases were categorized as stages V/VIC of Braak and Braak (1, 47). Concomitant Lewy body disease occurred in no case. Control cases (non-AD) did not show neurological or metabolic disease, and the neuropathological examination, carried out in similar regions and with the same methods as in AD cases, did not show lesions. In particularly, no amyloid or tau deposits were seen in the regions examined. Therefore, cases with AD-related changes corresponding to stages I to III of Braak and Braak were not considered in the present study.

In addition, paraformaldehyde-fixed sections of the HF from 2 epileptic patients with hippocampal sclerosis who had undergone an anterior temporal lobectomy at the Neurosurgery Department of the "La Princesa" Hospital (Madrid, Spain) (Table) (see ref. [48] for technical details) were included in this study.

Antibodies

Several antibodies against Nogo proteins were used: a polyclonal antibody against amino acids 223–399 of human Nogo-A (Gen Bank Accession No. KIAA0886, diluted 1:2000); a goat polyclonal antibody against Nogo, N-18, which recognizes Nogo-A, -B, and foocen (diluted 1:200 from Santa Cruz Biotechnology, Santa Cruz, CA); and a monoclonal antibody (NG1) against Nogo-A (49). The following primary antibodies were also used: a mouse monoclonal antibody against glial fibrillary acidic protein (GFAP, diluted 1:500, Chemicon, Temecula, CA) to label astrocytes; a mouse monoclonal antibody against MBP (Chemicon) to label the myelin protein (diluted 1:500 for Western blot and 1:250 for immunohistochemistry); a monoclonal antibody against a nonapeptide epitope derived from the hemaglutinin protein of human influenza virus (HA, diluted 1:1000, clone 12CA5; Roche Applied Science, Indianapolis, IN); a rabbit polyclonal antibody against human neuronal specific enolase (NSE, diluted 1:200, Dako, Glostrup, Denmark); a monoclonal antibody against human β-amyloid (1–17) (clone 6E10, diluted 1:500, Sigma, St. Louis, MO). Finally, a rabbit polyclonal antibody against carnosine (β−alanyl-L-histidine) (CAR, diluted 1:400; kindly provided by F.L. Margolis, Baltimore, MD) was used to label oligodendrocytes (50, 51).

Western Blotting and Immunoprecipitation Techniques

Human postmortem tissue samples from frontal cortex (area 8) and hippocampal formation (Table) were homogenized (10% w/v) in ice-cold Tris-saline buffer (50 mM Tris-HCl, 150 mM NaCl, pH 7.4) containing 0.5% (w/v) Triton X-100, 0.5% (w/v) Nonidet P-40 (Igepal, Sigma) and 1× cocktail of protease and phosphatase inhibitors (HB buffer) (52), using a motor-driven glass-teflon homogenizer in ice. The homogenate was clarified by centrifugation at 13,000 × *g* for 15 minutes, and the protein contents of soluble fractions were determined using the Bio-Rad detergent-compatible assay (Bio-Rad, Hercules, CA). Tissue extracts (i.e. 10 μg for MBP or 30 μg for Nogo-A samples) were boiled in Laemmli sample buffer at 100°C for 10 minutes, followed by 6 to 10% SDS-PAGE, and electro-transferred to nitrocellulose membranes (Amersham Biosciences, Little Chalfont, UK) for 6 hours. Following transfer, membranes were incubated overnight at 4°C with either α-Nogo-A antibody (N-18, 1:200 diluted (53), α-NSE [1:200 diluted], or α-MBP [1:500 diluted]). Membranes were subsequently incubated with peroxidase-tagged secondary antibodies (α-IgG raised in goat, rabbit, or mouse, respectively, Dako) and peroxidase activity was visualized using the ECL-plus kit (Amersham Biosciences). Cell extracts from Nogo-A transfected COS1 cells were used as an internal control. Quantification of the density of bands of Western blots was performed using the Bio-Rad Quantity One Image software (Bio-Rad). Films were scanned at 1,200 x 1,200 dpi resolution and the densitometric values (from 0 to 255) of labeled bands were determined. The ratio of Nogo-A or MBP bands to NSE was then calculated for each AD and non-AD sample. The Student *t*-test was used to assess statistical significance.

For immunoprecipitation, brain lysates from AD patients (Table) were incubated with 1 μg of α-Nogo A or α-Aβ or pre-immune serum at 4°C overnight. This mixture was subsequently incubated with Protein G beads (Sigma) for 2 to 4 hours at 4°C. The beads were washed 3 times, once in 20 mM Tris buffer, pH 7.5, containing 150 mM NaCl, 1 mM $CaCl_2$, 1 mM $MgCl_2$, 1% Triton X-100, protease and phosphatase inhibitors, and twice in the same buffer containing only 0.1% Triton X-100. The beads were re-suspended in SDS-PAGE loading buffer, boiled, and analyzed by Western blot.

Characterization of α-Nogo-A Antibodies

COS1 cells were maintained in culture with Dulbeccós modified Eagle's medium, supplemented with 10% fetal bovine serum, glutamine, and antibiotics (all purchased from GIBCO Life Technologies, Paisley, UK). Cells were grown in 35-mm-diameter 6-well multiplates (Nunc, Roskilde, Denmark) containing 10-mm-diameter glass coverslips at 60 to 70% confluence and transiently transfected with N-terminal HA-tagged human RTN4-A/Nogo-A (pCAGGS-HA-RTN-XS, [54]) or human RTN4-B/Nogo-B (pCMV-ASY/Nogo-B [55]) using Lipofectamine-Plus reagents according to the manufacturer's instructions (GIBCO Life Technologies). Seventy-two hours later, the coverslips were removed from the culture plate and fixed in 1% buffered paraformaldehyde (15 minutes,

© 2006 American Association of Neuropathologists, Inc.

Downloaded from http://jnen.oxfordjournals.org/ by guest on October 8, 2016

Copyright © 2006 by the American Association of Neuropathologists, Inc. Unauthorized reproduction of this article is prohibited.

4°C), rinsed in PBS 0.1M, pH 7.2–7.5, and stored. The remaining cells were scraped and harvested in Laemmli sample buffer. Cell extracts were separated by 6 to 10% SDS-PAGE electrophoresis, electro-transferred to nitrocellulose membranes and immunoblotted. Parallel coverslips were permeabilized with 0.1 M PBS containing 0.5% Triton X-100 for 15 minutes, blocked with normal goat serum, and sequentially incubated with primary antibodies for 2 hours at 30°C and then for 1 hour with Alexa Fluor-tagged secondary antibodies. After rinsing in PBS, cells were stained with Bisbenzimide (Hoescht 32444, 1 μM in PBS 0.1M, for 10 minutes), rinsed, and mounted in Fluoromount (Vector Labs, Burlingame, CA). In addition, primary antibodies were also checked on Western blots of brain protein extracts from newborn mice obtained in HB buffer as above.

Immunohistochemical Techniques

Sections (40- to 50-μm-thick) were obtained in a freezing microtome (Leica, Wetzlar, Germany) and processed. For immunohistochemistry, the sections were processed a follows: after rinsing in 0.1 M PBS, endogenous peroxidase activity was inhibited by a solution of 10% methanol and 3% hydrogen peroxide for 25 to 30 minutes. After blocking in a solution containing 10% normal serum for 2 hours, free-floating sections were incubated overnight with primary antibodies at

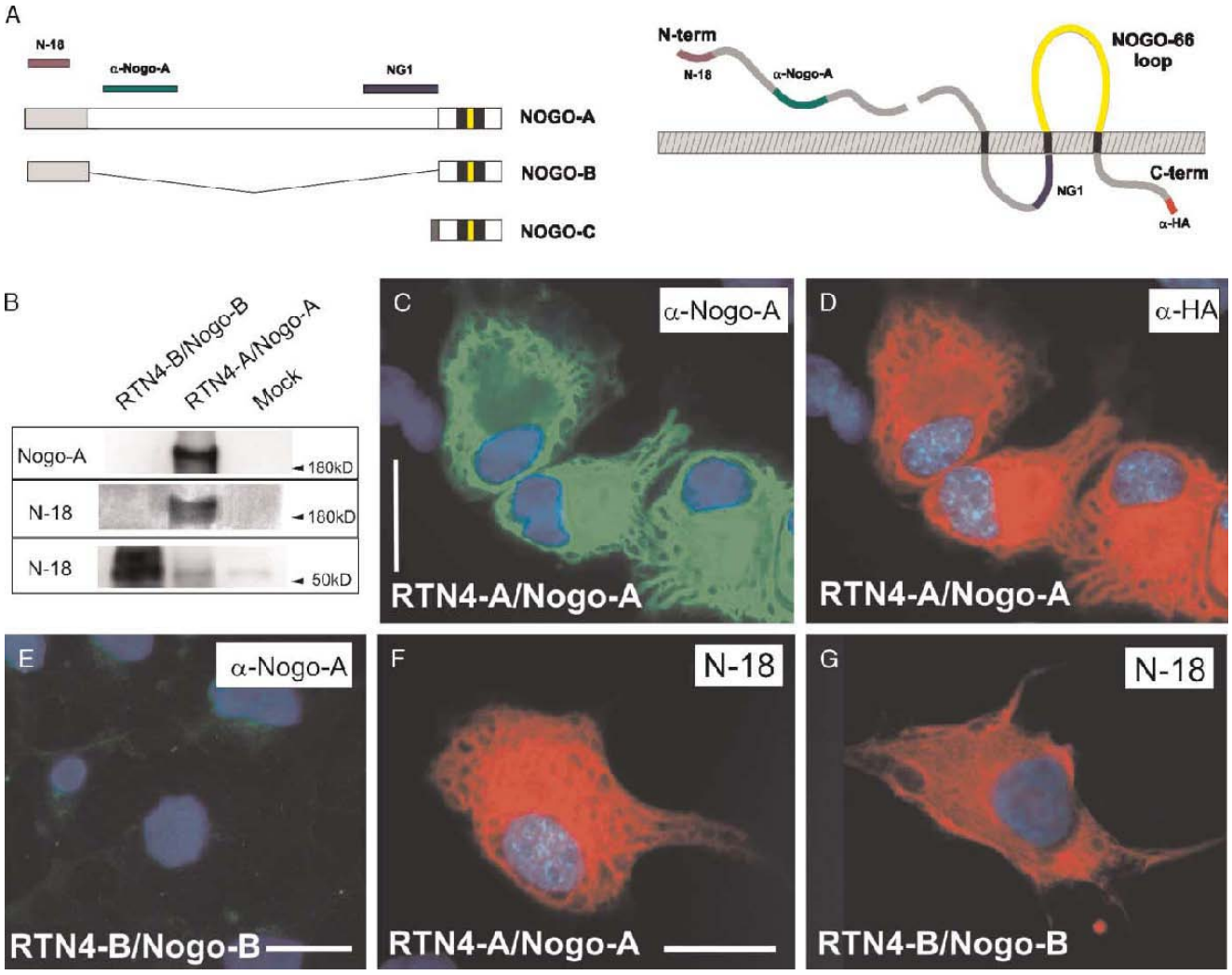

FIGURE 1. Recognition of Nogo-A by the antibodies used in the present study. **(A)** Localization of the Nogo-A regions detected by α-Nogo-A and N-18 antibodies. Note that the N-terminal region of the Nogo-A molecule has been schematized outside the cell, as was recently described by Dood et al (29). **(B)** Immunoblot of Nogo-A using α-Nogo-A and N-18 antibodies in cell extracts of RTN4-A/Nogo-A, RTN4-B/Nogo-B, and Mock-transfected cells. **(C–E)** Examples of COS1 cells transfected with RTN4-A/Nogo-A or RTN4-B/Nogo-B and immunostained with α-Nogo-A **(C, E)** and α-HA antibodies **(D)**. A lattice-like network characteristic of the endoplasmic reticulum is co-labeled with both antibodies following RTN4A/Nogo-A but not with RTN4B/Nogo-B. **(F, G)** COS1 transfected with RTN4-A/Nogo-A or RTN4-B/Nogo-B exhibited similar immunostaining with α-pan-Nogo (N-18) antibody. Scale bars = **(C)** 50 μm pertains to **(D)**; **(E)** 50 μm; **(F)** 50 μm pertains to **(G)**.

© 2006 American Association of Neuropathologists, Inc.

Downloaded from http://jnen.oxfordjournals.org/ by guest on October 8, 2016

Copyright © 2006 by the American Association of Neuropathologists, Inc. Unauthorized reproduction of this article is prohibited.

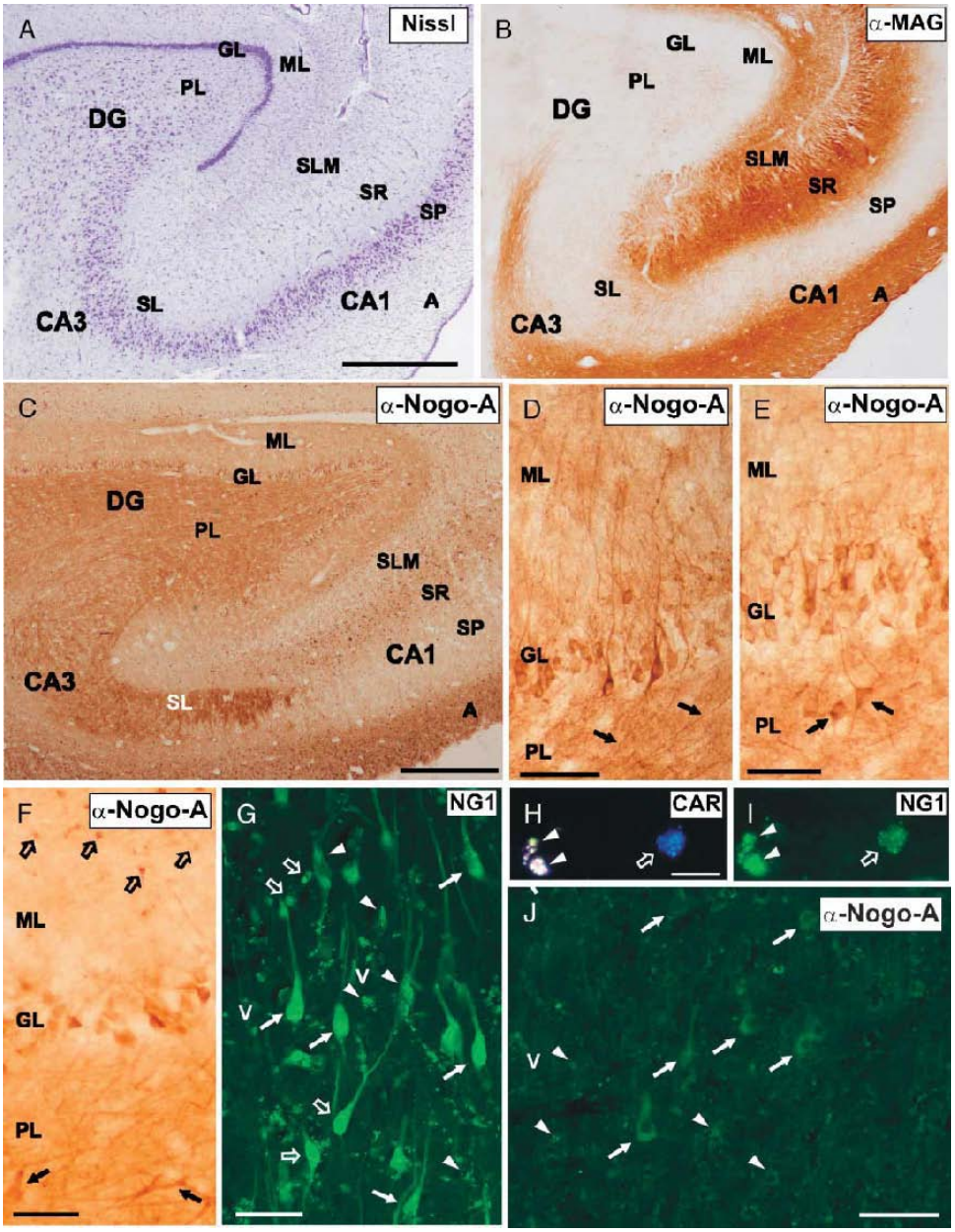

FIGURE 2. Topographical and cellular localization of Nogo-A in adult human hippocampal formation and frontal cortex. (**A, B**) Nissl staining **(A)** and panoramic distribution of MAG **(B)** in the hippocampus of a 73-year-old control patient. **(C)** Low-power photomicrograph of the hippocampus illustrating the distribution of Nogo-A immunoreactivity in the same case. Note the Nogo-A labeling in the granule cell layer of the dentate gyrus in the control hippocampus. **(D, E)** High-magnification photomicrographs illustrating details of Nogo-A immunoreactivity in the dentate gyrus. Granule cell axons (**[D]**, arrows) and some immunoreactive neurons displaying multipolar shapes (**[E]**, arrow) can be seen in the polymorphic cell layer. **(F)** High-magnification photomicrographs illustrating details of Nogo-A immunoreactivity in the dentate gyrus of a 53-year-old patient. Note the labeling of small cells (open arrows) of the SLM and large multipolar cells (arrows) in the polymorphic layer. In contrast, granule cells exhibit lower Nogo-A immunostaining than in older individuals. **(G)** High-magnification photomicrographs illustrating Nogo-A immunoreactivity in the entorhinal cortex using the NG1 antibody of a 73-year-old patient. Note the intense labeling of pyramidal (arrows) and non-pyramidal neurons (open arrows), and the characteristic autofluorescence of lipid deposits in old human neurons (arrowheads). **(H, I)** High magnification illustrating a double-labeled (CAR/Nogo-A) oligodendrocyte (open arrow) in the entorhinal cortex using AMCA- and Alexa Fluor-tagged secondary antibodies. The autofluorescence lipid deposits (arrowheads) are also labeled. **(J)** Photomicrographs illustrating Nogo-A immunoreactivity in the frontal cortex, using the α-Nogo-A antibody, of a 71-year-old patient. Principal neurons (arrows) and lipid deposits (arrowheads) can be seen. A, alveus; CA1-3, cornus ammonis region 1–3; DG, dentate gyrus; EC, entorhinal cortex; GL, granule layer; ML, molecular layer; PL, polymorphic cell layer; S, subiculum, SL, stratum lucidum; SLM, stratum lacunosum-moleculare; SP, stratum pyramidale; SR, stratum radiatum. Scale bars = **(A)** 500 μm pertains to **(B)**; **(C)** 500 μm; **(D–J)** 50 μm.

© 2006 American Association of Neuropathologists, Inc.

Downloaded from http://jnen.oxfordjournals.org/ by guest on October 8, 2016

Copyright © 2006 by the American Association of Neuropathologists, Inc. Unauthorized reproduction of this article is prohibited.

4°C. All primary antibodies were diluted in 0.1M PBS containing 5% normal serum, 0.2% gelatin and 0.5% Triton X-100. Tissue-bound primary antibody was detected utilizing the ABC method (Vector Laboratories). Peroxidase activity was revealed using 0.03% DAB and 0.01% hydrogen peroxide. Afterwards, sections were mounted onto gelatinized slides, dehydrated, and cover-slipped with Eukitt (Merck, Darmstadt, Germany).

In sections processed for immunofluorescence, primary antibodies were detected with Alexa-Fluor 488-, Alexa-Fluor 568- (Molecular Probes, Eugene, OR) or AMCA-tagged secondary antibodies (Vector Laboratories). Sections were mounted on Fluoromount and analyzed with a Leica Confocal microscope (TCS SPII, Leica).

Immunocytochemical controls, including omission of the primary antibody or its substitution by normal serum, prevented immunostaining in sections from non-AD and AD brains. For quantitative study, the mean number of Nogo-A-positive pyramidal cells in a 500-μm segment of the pyramidal layer in the CA2 and CA3 regions of consecutive sections (n = 3) of selected non-AD (3 cases) and AD (3 cases) as well as epileptic (2 cases) subjects was counted using a 40x oil immersion objective.

RESULTS

Characterization of α-Nogo-A Primary Antibodies

Immunoblot analysis using both α-Nogo-A and N-18 antibodies (Fig. 1), but not NG1 monoclonal antibody, detected a band of approximately 220 kDa in mouse brain extracts and in lysates of RTN4-A transfected COS1 cells (Fig. 1B). However, only N-18 identified a band of approximately 80 kDa in RTN4-B/Nogo-B transfected COS1 cells and the endogenous Nogo-B expressed in Mock and RTN4-B transfected COS1 cells of monkey kidney origin (Fig. 1B). In addition, COS1 cells transfected with HA-tagged RTN4-A/Nogo-A cDNA revealed an internal membrane staining pattern characteristic of the endoplasmic reticulum using antibodies against Nogo-A and NG1 (Fig. 1C). This labeling strongly matches the distribution pattern of the HA-epitope of the fusion protein revealed by the α-HA antibody (Fig. 1D), thus indicating that the α-Nogo-A antibody recognizes the HA-tagged RTN4-A/Nogo-A protein. Similar results were obtained using the N-18 antibody from Santa Cruz (Fig. 1F) and the monoclonal NG1 (see Fig. 2G for labeling in human tissue). However, diffuse fluorescence labeling by α-Nogo-A or NG1 was observed when COS1 cells were transfected with RTN4-B/Nogo-B (Fig. 1E), in contrast to those labeled by the N-18 antibody (Fig. 1G). Taken together, these results demonstrate that the antibodies against Nogo-A used in the present study exclusively recognize Nogo-A in humans and rodents.

Nogo-A Expression in Normal Aging and in AD Hippocampal Formation

To improve the definition of laminar boundaries, some sections parallel to those used for Nogo-A immunocytochemistry were either immunostained with the α-MAG antibody or Nissl-stained (Fig. 2A, B). The cell pattern and distribution of Nogo-A immunolabeling in tissue samples of human hippocampi was highly sensitive during postmortem and paraformaldehyde fixation. Postmortem times longer than 6 to 7 hours prior to autopsy, or prolonged paraformaldehyde fixation (more than 4 to 5 days), significantly decreased neuronal Nogo-A staining. For example, in cases AD_{122} and non-AD_{22} (Table), where paraformaldehyde fixation lasted more than 10 to 15 days, Nogo-A was limited to small cells (oligodendrocytes, see below) in the white matter (Supplementary Fig. 1).

The pattern of Nogo-A immunostaining in the human hippocampal formation of aged cases was similar to that reported in adult rodents (53). Thus, Nogo-A immunoreactivity was prominent in the white matter and fimbria, as well as in neural parenchyma of both the entorhinal cortex and hippocampus, which matched the distribution of myelinated fiber tracts in the hippocampus, as determined by MAG labeling (Fig. 2B). Both principal and non-pyramidal neurons were immunolabeled with α-Nogo-A antibody, as well small-sized cells (8- to 10-μm-diameter main axis) resembling oligodendrocytes (Fig. 2). This was confirmed by double fluorescence labeling using α-Carnosine (a oligodendrocyte marker (56, 57) and α-Nogo-A antibodies (Fig. 2H, I).

Interestingly, numerous, but not all, granule cells in the dentate gyrus were also immunostained, displaying a Golgi-like pattern with apical dendrites expanding into the molecular layer (Fig. 2C–E). Moreover, mossy fiber projections were particularly immunolabeled (Fig. 2C). A detailed analysis of Nogo-A immunoreactivity in granule cells indicated a moderate increase in older (>65 years) than in middle-aged (50 years) cases (Fig. 2D, E). In addition, a few pyramidal neurons in the hippocampus proper (CA1-3) were slightly immunostained, with increasing numbers in the subiculum and the adjacent entorhinal cortex (Fig. 2G), as well as in the frontal cortex (Fig. 2J). This pattern was obtained equally using either α-Nogo-A or NG1 antibodies. Lastly, Nogo-A-positive non-pyramidal neurons exhibiting multipolar, inverted-pyramidal or more irregular shapes were seen scattered in pyramidal, granule and polymorphic cell layers of the hippocampus, as well as in the entorhinal cortex (Fig. 2E). Taken together, these results corroborate that Nogo-A is expressed in neurons and oligodendrocytes in the human hippocampal formation.

The distribution pattern for Nogo-A-immunoreactive elements in the hippocampal formation in AD was similar to that observed in normal aging with the white matter, granule cells, and mossy fiber projections clearly delineated. Moreover, oligodendrocytes were seen in both the stratum radiatum and stratum lacunosum-moleculare (Fig. 3). However, increased numbers of Nogo-A-positive polymorphic and pyramidal cells, especially in the CA3-2 regions, were seen in the AD hippocampus, in contrast to non-AD samples (30.6 ± 3.1 (AD) vs 5.1 ± 0.5 (non-AD; mean ± SDM) (Fig. 3B, C, E). This was also observed in the HF of epileptic patients (Fig. 3D, E). Increased Nogo-A expression by commissural/associative cells correlated with the prominent immunoreactivity found in the inner portion of the molecular layer of the dentate gyrus (Fig. 4A). In addition, increased numbers of

© 2006 American Association of Neuropathologists, Inc.

Downloaded from http://jnen.oxfordjournals.org/ by guest on October 8, 2016

Copyright © 2006 by the American Association of Neuropathologists, Inc. Unauthorized reproduction of this article is prohibited.

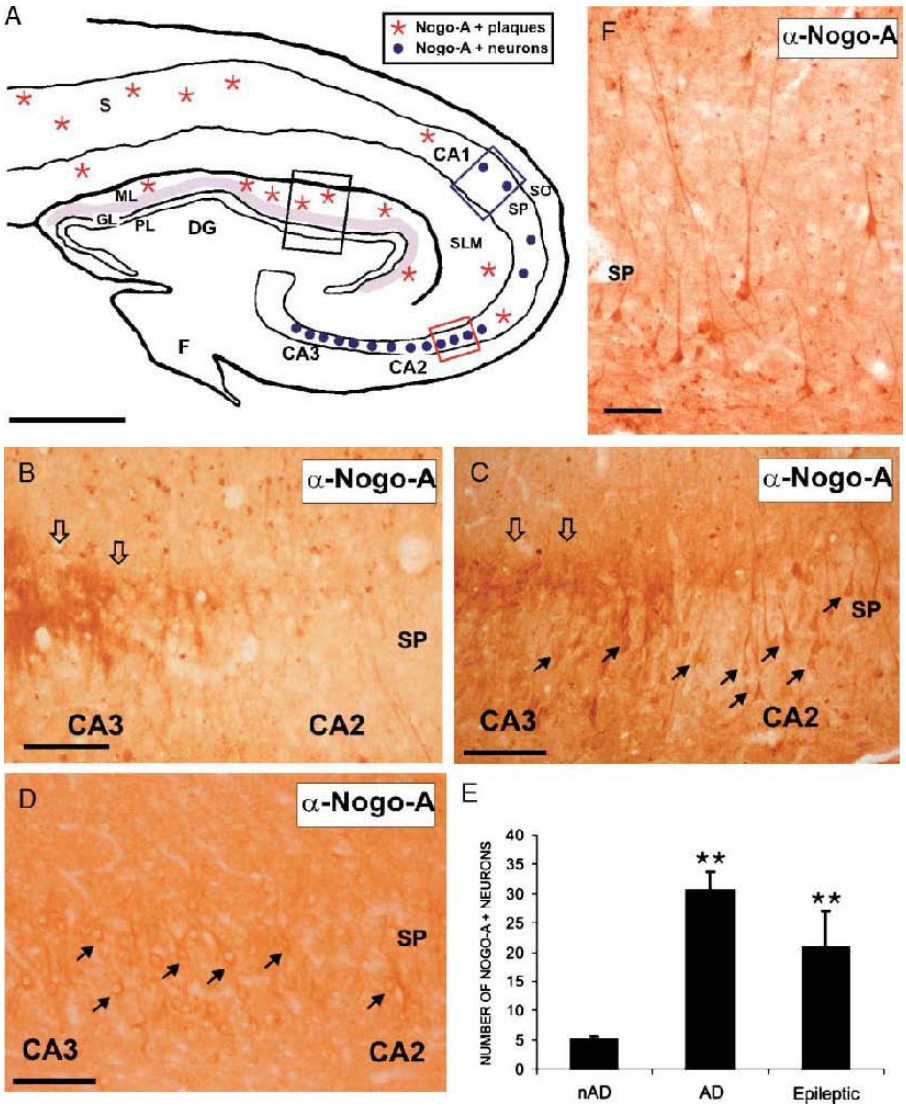

FIGURE 3. Nogo-A immunoreactivity in AD hippocampal formation. **(A)** Camera lucida drawing depicting the principal changes in Nogo-A-positive elements in the AD hippocampus. Blue dots represent Nogo-A-over-expressing pyramidal neurons in the CA3-2 region. Asterisks represent Nogo-A-containing deposits. The increased Nogo-A labeling of the inner molecular layer of the dentate gyrus in AD-affected hippocampi is labeled in violet (see Results for details). **(B, C)** High-magnification photomicrographs of the red-boxed area in **(A)** illustrating details of Nogo-A immunoreactivity in the CA3-2 region in control **(B)** and AD **(C)** cases. Note the increased number of Nogo-A-immunoreactive pyramidal neurons in AD. Open arrows point to the mossy fiber projection in the SL of the CA3. **(D)** High-magnification photomicrograph illustrating details of Nogo-A immunoreactivity in the CA3-2 region in the epileptic hippocampus of a 43-year-old patient. Numerous Nogo-A-positive pyramidal cell (arrows) are labeled. **(E)** Quantification of Nogo-A-labeled cells in the CA2-3 regions of AD, age-matched controls (nAD) and epileptic patients. Quantitative data in histograms are expressed as the mean number of immunoreactive cells. Error bars correspond to the standard deviation of the mean (SDM). Asterisks indicate statistically significant differences between AD/epileptic and nAD (non-AD or age-matched controls) columns (**, $p < 0.05$; Student *t*-test) **(F)** Photomicrograph illustrating examples of Nogo-A-immunoreactive pyramidal cells localized in the blue-boxed region of **(A)**. A, alveus; CA1-3, cornus ammonis region 1–3; DG, dentate gyrus; EC, entorhinal cortex; GL, granule layer; ML, molecular layer; PL, polymorphic cell layer; S, subiculum, SL, stratum lucidum; SLM, stratum lacunosum-moleculare; SP, stratum pyramidale; SR, stratum radiatum. Scale bars = **(A)** 500 μm; **(B–D, F)** 75 μm.

pyramidal cells were also immunolabeled in the CA1 (Fig. 3G) and in the frontal cortex (Figs. 3G, 4C).

Strong Nogo-A immunoreactivity was also localized in neuritic plaques, as revealed with NG1 and α-Nogo-A antibodies in the hippocampus as well as in the entorhinal cortex (Fig. 4A, B, D–F). A quantitative study revealed that 64% of amyloid deposits in the HF were associated with Nogo-A-containing cellular processes. This labeling was not observed in immunocytochemical controls. However, Nogo-A did not co-immunoprecipitate with either Aβ or APP as determined in parallel experiments, a feature that suggest no physical interaction (Supplementary Fig. 2). Finally,

© 2006 American Association of Neuropathologists, Inc.

Copyright © 2006 by the American Association of Neuropathologists, Inc. Unauthorized reproduction of this article is prohibited.

Downloaded from http://jnen.oxfordjournals.org/ by guest on October 8, 2016

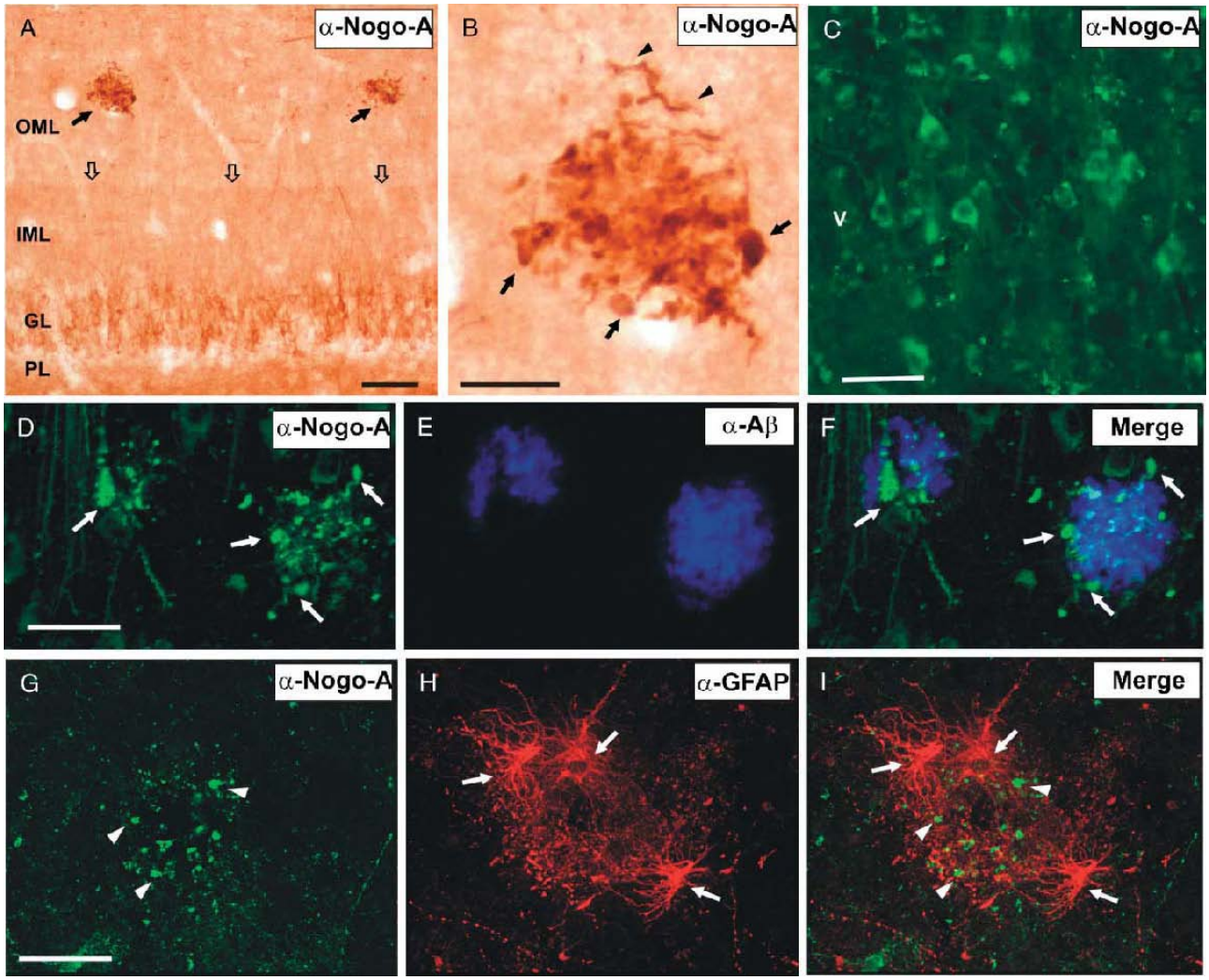

FIGURE 4. Nogo-A immunoreactivity around amyloid aggregates. **(A)** Low-power photomicrograph of the black-boxed area in Figure 3A illustrating the distribution of Nogo-A immunoreactivity in the dentate gyrus in AD sections. Note the intense Nogo-A labeling in the inner molecular layer (open arrows) and the presence of 2 large Nogo-A containing aggregates (arrows) in the outer molecular layer. **(B)** High-magnification photomicrograph illustrating details of Nogo-A-containing aggregates shown in **(A)**. Round (arrows) and dystrophic-immunoreactive (arrowheads) material can be seen. **(C)** High-magnification photomicrographs illustrating details of Nogo-A immunoreactivity in the frontal cortex of a 71-year-old case with AD. **(D–F)** High-magnification illustrating a double-labeled (Aβ/Nogo-A) aggregate in the subiculum. Nogo-A-immunoreactive material (**[D, F]**, arrows) is not labeled with the Aβ antibody. **(G–I)** High-power photomicrograph illustrating a double-labeled (GFAP/Nogo-A) aggregate in the hippocampus. Nogo-A-immunoreactive material (arrowheads in G and I) is not labeled with GFAP antibody (**[H, I]**, arrows). A, alveus; CA1-3, cornus ammonis region 1–3; DG, dentate gyrus; EC, entorhinal cortex; GL, granule layer; ML, molecular layer; PL, polymorphic cell layer; S, subiculum, SL, stratum lucidum; SLM, stratum lacunosum-moleculare; SP, stratum pyramidale; SR, stratum radiatum. Scale bars = **(A)** 100 μm; **(B–C)** 50 μm; **(D,G)** 50 μm pertains to **(E, F)** and **(H, I)**, respectively.

double-labeled sections using α-GFAP and α-Nogo-A antibodies exhibited amorphous Nogo-A-immunoreactive, GFAP-negative material surrounded by GFAP-positive astroglial cells (Fig. 4G–I).

Quantitative Western Immunoblot Analysis of Nogo-A and MBP in AD Hippocampal Formation and Frontal Cortex

Several authors have described increased Nogo-A expression in brain syndromes or diseases (34, 40).Therefore, we investigated whether differences in Nogo-A cellular expression in AD when compared with age-matched controls correlated with the total Nogo-A protein content (Fig. 5). Immunoblot analysis using the α-Nogo-A antibody detected a band of 200 to 210 kDa in protein extracts from human hippocampi and frontal cortices (AD and non-AD) (Fig. 5A). In these experiments, nitrocellulose membranes were also immunoblotted to determine NSE levels and thereby correlate them to Nogo-A and/or to MBP protein. Densitometric analyses were focused on the 200- to 210-kDa band of

© 2006 American Association of Neuropathologists, Inc.

Downloaded from http://jnen.oxfordjournals.org/ by guest on October 8, 2016

Copyright © 2006 by the American Association of Neuropathologists, Inc. Unauthorized reproduction of this article is prohibited.

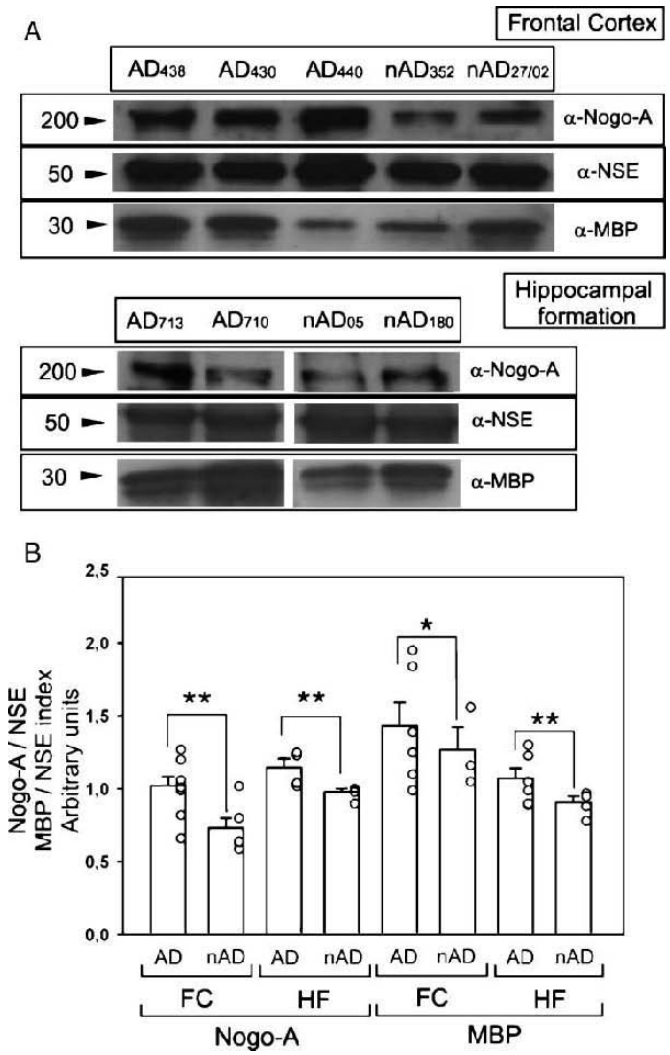

FIGURE 5. Changes in Nogo-A protein levels in the human cortex in AD samples. **(A, B)** Immunoblot of Nogo-A, NSE, and MBP protein levels in the frontal cortex and HF **(A)** and densitometric quantification **(B)** of labeled bands of protein extracts from aged-matched (nAD) (n = 6) and AD (n = 9) patients. Quantitative data in histograms are expressed as the mean of the ratio of Nogo-A or MBP optical density to NSE. Error bars correspond to the standard error. Each dot represents one experiment. Asterisks indicate statistically significant differences between columns (**, $p < 0.05$; *, $p < 0.1$; Student *t*-test)

Nogo-A, the 50-kDa band of NSE, and the 29-21-kDa band of MBP (see Material and Methods for details) (Fig. 5B). Increased Nogo-A protein levels were calculated in samples from frontal cortex and hippocampal formation. A significant increase in Nogo-A protein levels (1.4-fold increase in frontal cortex and 1.17-fold increase in HF; $p < 0.05$, Student *t*-test) was observed in AD compared with age-matched controls (Fig. 5B), thus supporting the view that Nogo-A is over-expressed in AD. MBP protein levels were also increased (1.14-fold increase in frontal cortex; and 1.19-fold increase in HF; $p < 0.1$ and $p < 0.05$, respectively, Student *t*-test) in AD compared with age-matched controls (Fig. 5B).

DISCUSSION

Myelin-Associated Proteins in Human Hippocampal Formation in Normal Aging and in Alzheimer Disease

We have studied the expression of Nogo-A in normal aging and in AD by using immunocytochemical and Western blotting techniques. Since different results have been published for human samples (33, 34), special care was taken to establish the specificity of the primary α-Nogo-A antibodies used in the present study. The specificity of the primary antibodies was verified by Western blots of brain extracts, as well as by immunostaining of cells transfected with cDNAs encoding human RTN4-A/Nogo-A or RTN4-B/Nogo-B.

The adult distribution patterns of Nogo-A immunoreactivity and cell staining with α-Nogo-A and the NG1 antibodies in aged human hippocampal formation were similar but not identical to those reported in mouse (27, 53) and rats (58). In addition, our results were slightly different than those recently described by Bandtlow et al, where little or no neuronal staining was noted in 30-to 40-year-old human hippocampi (34), but contradictory to reported by Buss et al, who found no labeling of granule and pyramidal cells in the human hippocampus from individuals of 70 to 80 years of age (33). However, we obtained similar results to Bandtlow et al, in epileptic hippocampal sections immunostained with our α-Nogo-A antibody. Thus, these minor differences between the results published by Bandtlow and our own (e.g. granule cell labeling) may reflect age-related changes in the hippocampal circuitry (see below) with increased Nogo-A expression in older subjects. Nevertheless, we believe that the discrepancies between our study and that of Buss et al can be attributed to differences in sample manipulation and/or immunocytochemical procedures, because the work of Buss et al was carried out in paraffin sections in which antigenicity might have been reduced. In fact, our preliminary studies had shown that paraffin embedding largely reduces Nogo-A immunoreactivity (unpublished observations). Similar discrepancies have been reported during the characterization of Nogo-A-immunoreactive elements in rodent CNS. Two studies have shown absence of neuronal Nogo-A staining (27, 49). However, Nogo-A immunoreactivity in neurons and oligodendrocytes has been extensively described by several groups and in several species (mice and rats [27, 53, 58], Xenopus [59], and humans [40]), and it has been recently characterized by Dood et al (29). Moreover, it is relevant that Nogo-A is localized in the soma of the granule cells and their axons: for example, the mossy fibers, a non-myelinated connection in humans (Fig. 2). This also occurs in sclerotic and non-sclerotic epileptic hippocampi ([34] and present results). Together, these findings support the hypothesis that Nogo-A may have different roles, including participation in neuronal survival and synaptic

© 2006 American Association of Neuropathologists, Inc.

Downloaded from http://jnen.oxfordjournals.org/ by guest on October 8, 2016

Copyright © 2006 by the American Association of Neuropathologists, Inc. Unauthorized reproduction of this article is prohibited.

remodeling or stabilization, in addition to those associated with myelin formation and stabilization.

Functions of Myelin-Associated Proteins in AD

A recent study by Tian et al reported that 63.5% of patients with autopsy-confirmed AD displayed a decrease in white matter, particularly in the occipital cortex (60). Although a detailed study of a putative decrease in the white matter was not addressed in the present study, we showed an increase in Nogo-A and a slight increase in MBP protein in the frontal cortex and the HF in advanced AD (stages V/VI of Braak and Braak). As indicated above, Nogo-A is expressed in neurons as well as in oligodendrocytes; in contrast, MBP can be over-expressed by reactive oligodendrocyte progenitors and reactive oligodendrocytes. In addition, it has been reported that, under certain circumstances, a demyelination in the adult CNS can be followed by a considerable degree of repair, at least for several axonal tracts (the cerebellar peduncle), in which axons are invested with new myelin sheaths (61, 62). Thus, the over-expression of certain myelin-associated proteins (e.g. MBP) may form part of the oligodendrocyte responses to axonal impairment, aimed to direct the restoration of myelin sheaths and functional neuronal recovery. Increased expression of myelin-associated proteins (MBP) mRNA in AD has already been reported (45). In the present study, we were unable to distinguish specific over-expression of Nogo-A or MBP in oligodendrocytes. However, we showed by Western blotting that MBP protein levels are slightly increased in AD. This over-expression confirms recent studies reporting the over-expression of other myelin-associated proteins such as MAG and MBP in reactive oligodendrocytes following ischemia (63), CNS lesions (27, 64-66), and in the demyelinating lesions in multiple sclerosis or familial amyotrophic lateral sclerosis (39, 40). While the biological effects of MBP over-expression in several patients remain unknown, we can hypothesize that increased myelin protein synthesis in surviving oligodendrocytes may constitute an attempt to repair affected myelin tracts, as suggested by Jensen et al in the hippocampus following EC lesions (64, 65). In contrast, Nogo-A over-expression in neurons may reflect functions other than myelin stabilization.

A large number of intracellular interactions have been attributed to Reticulon protein family members (22). For example, Nogo-A co-immunoprecipitates with cytoskeletal (α-tubulin) (67), mitochondrial (68), and myelin (MBP) proteins (67), as well as with anti-apoptotic members of the Bcl-2 protein family (54). In addition, members of the Reticulon protein family play relevant roles in the vesicular trafficking of proteins from the endoplasmic reticulum to other intracellular compartments such as the Golgi complex and endosomes (69). Taken together, these findings indicate that Nogo proteins contribute to neuronal physiology and cellular homeostasis.

As mentioned above, we demonstrated increased Nogo-A immunoreactivity by pyramidal cells in the CA3-2 region of the hippocampus in AD when compare with age-matched controls. The entorhino-hippocampal connections are reduced during normal aging, but they are particularly affected in AD, since extensive loss of projecting neurons from layers II to III of the entorhinal cortex occurs in affected brains (3). In addition, transneuronal cell death of granule cells occurs following entorhinal lesions in experimental animals models (70). In AD brains, axon sprouting from commissural/associative connections increases positive feedback in the dentate gyrus following entorhinal cell loss (71, 72). In addition, Nogo-A and its receptor have been localized in synaptic contacts (27, 29, 73) and the blockade of Nogo-A enhances axonal sprouting in neurons (36, 74, 75). Finally, a fast but transient decrease in Nogo-A expression in cells undergoing axonal sprouting has been reported in lesioned hippocampi (35, 37, 53). Conversely, Nogo-A over-expression has been determined in axotomized neurons (Lam et al, 2005, Soc Neurosci Abstract, A.M. and J.A.D.R., unpublished results). Axonal sprouting and synaptic reorganization also occur in the hippocampus in cases with temporal epilepsy, where severe hippocampal degeneration is often observed, and where increased Nogo-A protein levels have been noted from early non-sclerotic stages (34). While the exact role of Nogo-A in these events is unknown, an interesting possibility which needs further study, is that Nogo-A expression may increase in the neuron after its sprouting process takes place. Thus, delayed Nogo-A over-expression may contribute to reactive synapse formation in AD, perhaps by providing additional synaptic stability beyond the decline predicted from cell loss.

Myelin-Associated Proteins and Aβ Plaque Formation

In the present study, we described the presence of Nogo-A in neuritic plaques in the hippocampus of AD. These findings are in agreement with the observation of Nogo-A in the vicinity of Aβ deposits in transgenic mice bearing the APP-Swedish mutation (Prinjha et al, 2003, Soc Neurosci Abstract). However, we were unable to co-immunoprecipitate Nogo-A with Aβ or APP in AD-affected brains although we used several antibodies (Supplementary Fig. 2). Taken together, these results open challenging questions as whether Nogo-A expression is modulated by Aβ or their participation in the neurotoxic effect of Aβ. Interestingly, a recent study by He et al reported that both RTN3 and RTN4-B (Nogo-B) interact with BACE1 (β-secretase), increasing Aβ production when they were over-expressed (76). Taken together, these results indicate that members of Reticulon proteins may play a role in APP-processing, as well as in Aβ plaque formation, both of which warrant further analysis. In conclusion, we believe that our study reinforces the hypothesis that Reticulon proteins such as Nogo-A participate in cell responses occurring in AD, thus opening the possibility to consider these proteins as new putative drug targets in AD, as recently suggested in other neurodegenerative disorders (77).

ACKNOWLEDGMENTS

The authors thank Dr. J. de Felipe and Dr. J. Arellano (Instituto Cajal, CSIC, Madrid) for providing hippocampal

© 2006 American Association of Neuropathologists, Inc.

Downloaded from http://jnen.oxfordjournals.org/ by guest on October 8, 2016

Copyright © 2006 by the American Association of Neuropathologists, Inc. Unauthorized reproduction of this article is prohibited.

sections from epileptic patients for this study. The authors also thank Prof. Y. Tsujimoto (Department of Medical Genetics, Osaka University Graduate Scholl of Medicine, Osaka, Japan) for providing the HA-tagged human RTN4-A/Nogo-A expression vector; Dr. M. Yutsudo (Research Institute for Microbial Diseases, Osaka University, Osaka, Japan) for providing the RTN4-B/Nogo-B cDNA; and Dr. FL Margolis (Department of Anatomy and Neurobiology, University of Maryland, Baltimore, MD) for providing the antibody against Carnosine. We are also grateful to M López and E Márquez, for technical assistance, as well as R. Rycroft for editorial advice.

REFERENCES

1. Braak H, Braak E. Evolution of neuronal changes in the course of Alzheimer's disease. J Neural Transm Suppl 1998;53:127–40
2. Selkoe DJ. Translating cell biology into therapeutic advances in Alzheimer's disease. Nature 1999;399:A23–31
3. Braak H, Del Tredici K, Schultz C, et al. Vulnerability of select neuronal types to Alzheimer's disease. Ann N Y Acad Sci 2000;924:53–61
4. Lorenzo A, Yankner BA. Amyloid fibril toxicity in Alzheimer's disease and diabetes. Ann N Y Acad Sci 1996;777:89–95
5. Kowall NW, McKee AC, Yankner BA, et al. In vivo neurotoxicity of beta-amyloid (beta(1–40)) and the beta(25–35) fragment. Neurobiol Aging 1992;13:537–42
6. Suhara T, Magrane J, Rosen K, et al. Abeta42 generation is toxic to endothelial cells and inhibits eNOS function through an Akt/GSK-3beta signaling-dependent mechanism. Neurobiol Aging 2003;24:437–51
7. Xu J, Chen S, Ahmed SH, et al. Amyloid-beta peptides are cytotoxic to oligodendrocytes. J Neurosci 2001;21:RC118
8. Whitman GT, Cotman CW. Oligodendrocyte degeneration in AD. Neurobiol Aging 2004;25:33–36
9. Noble M. The possible role of myelin destruction as a precipitating event in Alzheimer's disease. Neurobiol Aging 2004;25:25–31
10. Wallin A, Gottfries CG, Karlsson I, et al. Decreased myelin lipids in Alzheimer's disease and vascular dementia. Acta Neurol Scand 1989;80:319–23
11. Wilkins A, Chandran S, Compston A. A role for oligodendrocyte-derived IGF-1 in trophic support of cortical neurons. Glia 2001;36:48–57
12. Wilkins A, Majed H, Layfield R, et al. Oligodendrocytes promote neuronal survival and axonal length by distinct intracellular mechanisms: a novel role for oligodendrocyte-derived glial cell line-derived neurotrophic factor. J Neurosci 2003;23:4967–74
13. Dai X, Lercher LD, Clinton PM, et al. The trophic role of oligodendrocytes in the basal forebrain. J Neurosci 2003;23:5846–53
14. McGeeAW, YangY, FischerQS, et al. Experience-driven plasticity of visual cortex limited by myelin and Nogo receptor. Science 2005;309:2222–26
15. Prinjha R, Moore SE, Vinson M, et al. Inhibitor of neurite outgrowth in humans. Nature 2000;403:383–84
16. GrandPre T, Nakamura F, Vartanian T, et al. Identification of the Nogo inhibitor of axon regeneration as a Reticulon protein. Nature 2000;403:439–44
17. Chen MS, Huber AB, van der Haar ME, et al. Nogo-A is a myelin-associated neurite outgrowth inhibitor and an antigen for monoclonal antibody IN-1. Nature 2000;403:434–39
18. McKerracher L, David S, Jackson DL, et al. Identification of myelin-associated glycoprotein as a major myelin-derived inhibitor of neurite growth. Neuron 1994;13:805–11
19. Mukhopadhyay G, Doherty P, Walsh FS, et al. A novel role for myelin-associated glycoprotein as an inhibitor of axonal regeneration. Neuron 1994;13:757–67
20. Kottis V, Thibault P, Mikol D, et al. Oligodendrocyte-myelin glycoprotein (OMgp) is an inhibitor of neurite outgrowth. J Neurochem 2002;82:1566–69
21. Wang KC, Koprivica V, Kim JA, et al. Oligodendrocyte-myelin glycoprotein is a Nogo receptor ligand that inhibits neurite outgrowth. Nature 2002;417:941–44
22. Oertle T, Schwab ME. Nogo and its paRTNers. Trends Cell Biol 2003;13:187–94
23. Park JB, Yiu G, Kaneko S, et al. A TNF Receptor Family Member, TROY, Is a coreceptor with Nogo receptor in mediating the inhibitory activity of myelin inhibitors. Neuron 2005;45:345–51
24. Wang KC, Kim JA, Sivasankaran R, et al. P75 interacts with the Nogo receptor as a co-receptor for Nogo, MAG and OMgp. Nature 2002;420:74–78
25. Shao Z, Browning JL, Lee X, et al. TAJ/TROY, an orphan TNF receptor family member, binds Nogo-66 receptor 1 and regulates axonal regeneration. Neuron 2005;45:353–59
26. Mi S, Lee X, Shao Z, et al. LINGO-1 is a component of the Nogo-66 receptor/p75 signaling complex. Nat Neurosci 2004;7:221–28
27. Wang X, Chun SJ, Treloar H, et al. Localization of Nogo-A and Nogo-66 receptor proteins at sites of axon-myelin and synaptic contact. J Neurosci 2002;22:5505–15
28. Jin WL, Liu YY, Liu HL, et al. Intraneuronal localization of Nogo-A in the rat. J Comp Neurol 2003;458:1–10
29. DoddD A, Niederoest B, Bloechlinger S, et al. Nogo-A, -B, and -C are found on the cell surface and interact together in many different cell types. J Biol Chem 2005;280:12494–12502
30. Josephson A, Widenfalk J, Widmer HW, et al. NOGO mRNA expression in adult and fetal human and rat nervous tissue and in weight drop injury. Exp Neurol 2001;169:319–28
31. Josephson A, Trifunovski A, Widmer HR, et al. Nogo-receptor gene activity: Cellular localization and developmental regulation of mRNA in mice and humans. J Comp Neurol 2002;453:292–304
32. Al Halabiah H, Delezoide AL, Cardona A, et al. Expression pattern of NOGO and NgR genes during human development. Gene Expr Patterns 2005;5:561–68
33. Buss A, Sellhaus B, Wolmsley A, et al. Expression pattern of NOGO-A protein in the human nervous system. Acta Neuropathol (Berl) 2005;110:113–19
34. Bandtlow CE, Dlaska M, Pirker S, et al. Increased expression of Nogo-A in hippocampal neurons of patients with temporal lobe epilepsy. Eur J Neurosci 2004;20:195–206
35. Josephson A, Trifunovski A, Scheele C, et al. Activity-induced and developmental downregulation of the Nogo receptor. Cell Tissue Res 2003;311:333–42
36. Blochlinger S, Weinmann O, Schwab ME, et al. Neuronal plasticity and formation of new synaptic contacts follow pyramidal lesions and neutralization of Nogo-A: A light and electron microscopic study in the pontine nuclei of adult rats. J Comp Neurol 2001;433:426–36
37. Meier S, Brauer AU, Heimrich B, et al. Molecular analysis of Nogo expression in the hippocampus during development and following lesion and seizure. Faseb J 2003;17:1153–55
38. Trifunovski A, Josephson A, Ringman A, et al. Neuronal activity-induced regulation of Lingo-1. Neuroreport 2004;15:2397–2400
39. Dupuis L, Gonzalez de Aguilar JL, di Scala F, et al. Nogo provides a molecular marker for diagnosis of amyotrophic lateral sclerosis. Neurobiol Dis 2002;10:358–65
40. Satoh J, Onoue H, Arima K, et al. Nogo-A and nogo receptor expression in demyelinating lesions of multiple sclerosis. J Neuropathol Exp Neurol 2005;64:129–38
41. Novak G, Kim D, Seeman P, et al. Schizophrenia and Nogo: elevated mRNA in cortex, and high prevalence of a homozygous CAA insert. Brain Res Mol Brain Res 2002;107:183–89
42. Gregorio SP, Mury FB, Ojopi EB, et al. Nogo CAA 3'UTR Insertion polymorphism is not associated with Schizophrenia nor with bipolar disorder. Schizophr Res 2005;75:5–9
43. Xiong L, Rouleau GA, Delisi LE, et al. CAA insertion polymorphism in the 3UTR of Nogo gene on 2p14 is not associated with schizophrenia. Brain Res Mol Brain Res 2005;133:153–56
44. Roher AE, Weiss N, Kokjohn TA, et al. Increased A beta peptides and reduced cholesterol and myelin proteins characterize white matter degeneration in Alzheimer's disease. Biochemistry 2002;41:11080–90
45. Macq AF, Goossens F, Maloteaux JM, et al. Overexpression of the myelin basic protein RNA in the cortex of a patient with Alzheimer's disease. Acta Neurol Belg 1989;89:316

© 2006 American Association of Neuropathologists, Inc.

Downloaded from http://jnen.oxfordjournals.org/ by guest on October 8, 2016

Copyright © 2006 by the American Association of Neuropathologists, Inc. Unauthorized reproduction of this article is prohibited.

46. Knopman D. Alzheimer type dementia. In: Dickson D, ed. *Neurodegeneration: Molecular pathology of dementia and movement disorders*. Basel: ISN, University Press, 2003:24–39
47. Braak H, Braak E. Temporal sequence of Alzheimer's disease-related pathology. In: PetersAMJ, ed. *Cerebral Cortex, Vol 14. Neurodegenerative and Related Changes in Structure and Function of Cerebral Cortex*. New York: Kluwer Academic/Plenum Publishers, 1999: 475–512
48. Alonso-Nanclares L, De Felipe J. Vesicular glutamate transporter 1 immunostaining in the normal and epileptic human cerebral cortex. Neuroscience 2005;134:59–68
49. Tozaki H, Kawasaki T, Takagi Y, et al. Expression of Nogo protein by growing axons in the developing nervous system. Brain Res Mol Brain Res 2002;104:111–19
50. De Marchis S, Melcangi RC, Modena C, et al. Identification of the glial cell types containing carnosine-related peptides in the rat brain. Neurosci Lett 1997;237:37–40
51. Marchis SD, Modena C, Peretto P, et al. Carnosine-related dipeptides in neurons and glia. Biochemistry (Mosc) 2000;65:824–33
52. Saez-Valero J, Sberna G, McLean CA, et al. Molecular isoform distribution and glycosylation of acetylcholinesterase are altered in brain and cerebrospinal fluid of patients with Alzheimer's disease. J Neurochem 1999;72:1600–1608
53. Mingorance A, Fontana X, Sole M, et al. Regulation of Nogo and Nogo receptor during the development of the entorhino-hippocampal pathway and after adult hippocampal lesions. Mol Cell Neurosci 2004;26:34–49
54. Tagami S, Eguchi Y, Kinoshita M, et al. A novel protein, RTN-XS, interacts with both Bcl-XL and Bcl-2 on endoplasmic reticulum and reduces their anti-apoptotic activity. Oncogene 2000;19:5736–46
55. Watari A, Yutsudo M. Multi-functional gene ASY/Nogo/RTN-X/RTN4: apoptosis, tumor suppression, and inhibition of neuronal regeneration. Apoptosis 2003;8:5–9
56. Biffo S, Grillo M, Margolis FL. Cellular localization of carnosine-like and anserine-like immunoreactivities in rodent and avian central nervous system. Neuroscience 1990;35:637–51
57. Artero C, Marti E, Biffo S, et al. Carnosine in the brain and olfactory system of amphibia and reptilia: A comparative study using immunocytochemical and biochemical methods. Neurosci Lett 1991;130:182–86
58. Huber AB, Weinmann O, Brosamle C, et al. Patterns of Nogo mRNA and protein expression in the developing and adult rat and after CNS lesions. J Neurosci 2002;22:3553–67
59. Klinger M, Diekmann H, Heinz D, et al. Identification of two NOGO/RTN4 genes and analysis of Nogo-A expression in Xenopus laevis. Mol Cell Neurosci 2004;25:205–16
60. Tian J, Shi J, Bailey K, et al. Relationships between arteriosclerosis, cerebral amyloid angiopathy and myelin loss from cerebral cortical white matter in Alzheimer's disease. Neuropathol Appl Neurobiol 2004;30:46–56
61. Yajima K, Suzuki K. Demyelination and remyelination in the rat central nervous system following ethidium bromide injection. Lab Invest 1979; 41:385–92
62. Blakemore WF. Remyelination of the superior cerebellar peduncle in the mouse following demyelination induced by feeding cuprizone. J Neurol Sci 1973;20:73–83
63. Gregersen R, Christensen T, Lehrmann E, et al. Focal cerebral ischemia induces increased myelin basic protein and growth-associated protein-43 gene transcription in peri-infarct areas in the rat brain. Exp Brain Res 2001;138:384–92
64. Jensen MB, Poulsen FR, Finsen B. Axonal sprouting regulates myelin basic protein gene expression in denervated mouse hippocampus. Int J Dev Neurosci 2000;18:221–35
65. Drojdahl N, Fenger C, Nielsen HH, et al. Dynamics of oligodendrocyte responses to anterograde axonal (Wallerian) and terminal degeneration in normal and TNF-transgenic mice. J Neurosci Res 2004;75:203–17
66. Mingorance A, Fontana X, Soriano E, et al. Over-expression of myelin-associated glycoprotein after axotomy of the perforant pathway. Mol Cell Neurosci 2005;29:471–83
67. Taketomi M, Kinoshita N, Kimura K, et al. Nogo-A expression in mature oligodendrocytes of rat spinal cord in association with specific molecules. Neurosci Lett 2002;332:37–40
68. Hu WH, Hausmann ON, Yan MS, et al. Identification and characterization of a novel Nogo-interacting mitochondrial protein (NIMP). J Neurochem 2002;81:36–45
69. Iwahashi J, Kawasaki I, Kohara Y, et al. Caenorhabditis elegans reticulon interacts with RME-1 during embryogenesis. Biochem Biophys Res Commun 2002;293:698–704
70. Kovac AD, Kwidzinski E, Heimrich B, et al. Entorhinal cortex lesion in the mouse induces transsynaptic death of perforant path target neurons. Brain Pathol 2004;14:249–57
71. Cotman CW, Anderson KJ. Synaptic plasticity and functional stabilization in the hippocampal formation: Possible role in Alzheimer's disease. Adv Neurol 1988;47:313–35
72. Scheff S. Reactive synaptogenesis in aging and Alzheimer's disease: lessons learned in the Cotman laboratory. Neurochem Res 2003;28: 1625–30
73. Liu YY, Jin WL, Liu HL, et al. Electron microscopic localization of Nogo-A at the postsynaptic active zone of the rat. Neurosci Lett 2003; 346:153–56
74. Buffo A, Zagrebelsky M, Huber AB, et al. Application of neutralizing antibodies against NI-35/250 myelin-associated neurite growth inhibitory proteins to the adult rat cerebellum induces sprouting of uninjured purkinje cell axons. J Neurosci 2000;20:2275–86
75. Emerick AJ, Neafsey EJ, Schwab ME, et al. Functional reorganization of the motor cortex in adult rats after cortical lesion and treatment with monoclonal antibody IN-1. J Neurosci 2003;23:4826–30
76. He W, Lu Y, Qahwash I, et al. Reticulon family members modulate BACE1 activity and amyloid-beta peptide generation. Nat Med 2004;10: 959–65
77. Bornebroek M, Kumar-Singh S. A novel drug target in Alzheimer's disease. Lancet 2004;364:1738–39

Downloaded from http://jnen.oxfordjournals.org/ by guest on October 8, 2016

© 2006 American Association of Neuropathologists, Inc.

Copyright © 2006 by the American Association of Neuropathologists, Inc. Unauthorized reproduction of this article is prohibited.

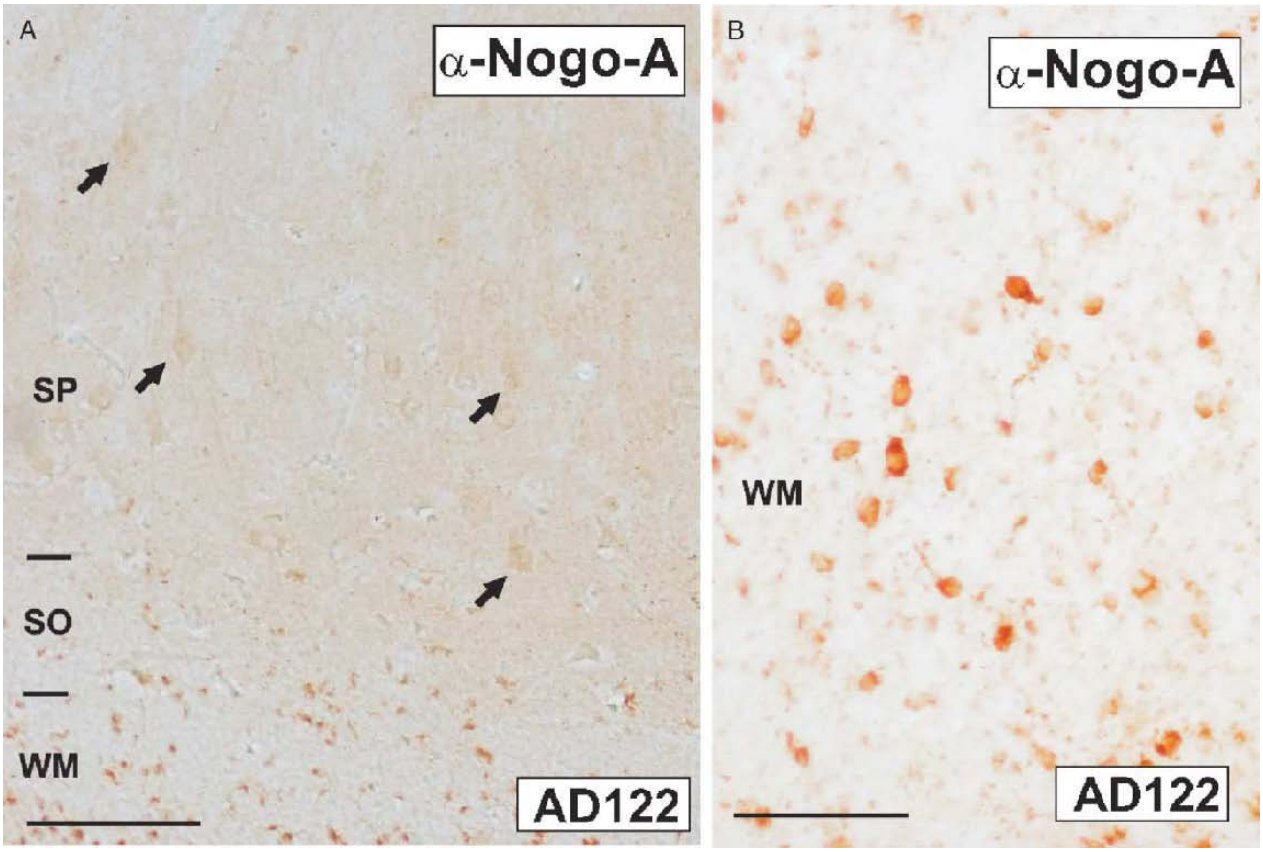

SUPPLEMENTARY FIGURE 1. Photomicrographs illustrating Nogo-A immunoreactivity in the hippocampus of a 75-year-old patient. Nogo-A can only be detected clearly in the oligodendrocytes present in the white matter but shows pale staining in principal neurons (interneurons and pyramidal cells) (**[A]**, arrows). Abbreviations: A, alveus; CA1-3, cornus ammonis region 1–3; DG, dentate gyrus; EC, entorhinal cortex; GL, granule layer; ML, molecular layer; PL, polymorphic cell layer; S, subiculum, SL, stratum lucidum; SLM, stratum lacunosum-moleculare; SP, stratum pyramidale; SR, stratum radiatum. Scale bars = **(A)** 100 mm; **(B)** 50 mm.

Downloaded from http://jnen.oxfordjournals.org/ by guest on October 8, 2016

Copyright © 2006 by the American Association of Neuropathologists, Inc. Unauthorized reproduction of this article is prohibited.

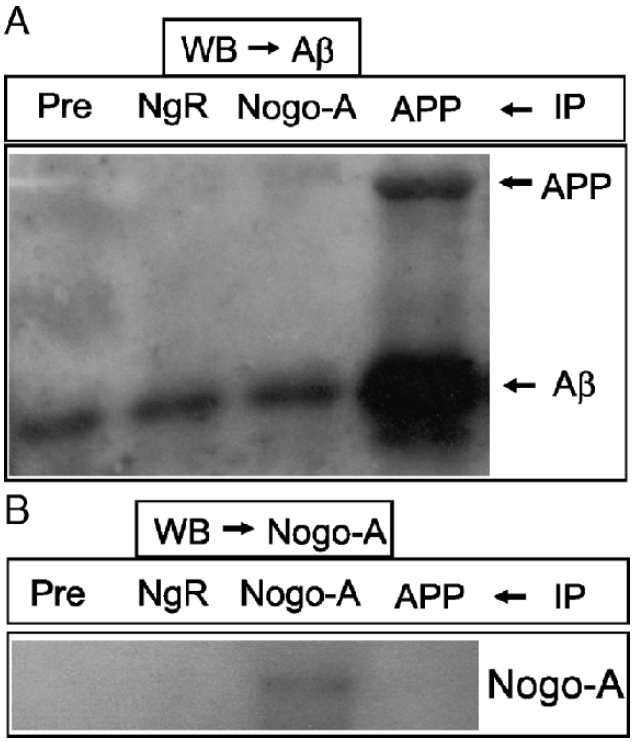

SUPPLEMENTARY FIGURE 2. Immunoblot of Aβ **(A)** and Nogo-A **(B)** after immunoprecipitation of AD proteins extracts (Table) with pre-immune serum (Pre), Nogo-A and APP antibodies. Nogo-A does not co-immunoprecipitate with Aβ **(A)** and APP **(B)**.

Downloaded from http://jnen.oxfordjournals.org/ by guest on October 8, 2016

Copyright © 2006 by the American Association of Neuropathologists, Inc. Unauthorized reproduction of this article is prohibited.